Journal of Computational Physics 355 (2018) 426–435

Contents lists available at ScienceDirect

Journal of Computational Physics

www.elsevier.com/locate/jcp

Spherical Bessel transform via exponential sum approximation of spherical Bessel function

Hidekazu Ikeno [a,b,*]

[a] NanoSquare Research Institute, Research Center for the 21st Century, Organization for Research Promotion, Osaka Prefecture University, 1-2 Gakuen-cho, Naka-ku, Sakai, Osaka 599-8570, Japan
[b] JST PRESTO, 4-1-8 Hon-cho, Kawaguchi, Saitama, 332-0012, Japan

ARTICLE INFO

Article history:
Received 11 June 2017
Received in revised form 11 November 2017
Accepted 13 November 2017
Available online 20 November 2017

Keywords:
Hankel transform
Spherical Bessel transform
Bessel function
Oscillatory integrals
Balanced truncation method

ABSTRACT

A new algorithm for numerical evaluation of spherical Bessel transform is proposed in this paper. In this method, the spherical Bessel function is approximately represented as an exponential sum with complex parameters. This is obtained by expressing an integral representation of spherical Bessel function in complex plane, and discretizing contour integrals along steepest descent paths and a contour path parallel to real axis using numerical quadrature rule with the double-exponential transformation. The number of terms in the expression is reduced using the modified balanced truncation method. The residual part of integrand is also expanded by exponential functions using Prony-like method. The spherical Bessel transform can be evaluated analytically on arbitrary points in half-open interval.

1. Introduction

In this paper, we consider the integrals transformation of a function $f(r)$ of the form,

$$\tilde{f}_l(k) = \int_0^\infty r^2 f(r) j_l(kr) dr \quad (k > 0), \tag{1}$$

where, $j_l(r)$ is the spherical Bessel function of the first kind of order l. The integral transformation (1) is referred as *a spherical Hankel* or *spherical Bessel transform* (SBT). The SBT appears when the Fourier transform of an angular momentum eigenfunction is considered. Let $\psi(\boldsymbol{r}) = f(r)Y_{lm}(\hat{\boldsymbol{r}})$, where $Y_{lm}(\hat{\boldsymbol{r}})$ is a spherical harmonic. Using the spherical wave expansion of plane wave,

$$e^{-i\boldsymbol{k}\cdot\boldsymbol{r}} = \sum_{l=0}^{\infty} (-i)^l j_l(kr) Y_{lm}(\hat{\boldsymbol{k}}) Y_{lm}^*(\hat{\boldsymbol{r}}), \tag{2}$$

then, the Fourier transform of $\psi(\boldsymbol{r})$ can be written as

* Correspondence to: NanoSquare Research Institute, Research Center for the 21st Century, Organization for Research Promotion, Osaka Prefecture University, 1-2 Gakuen-cho, Naka-ku, Sakai, Osaka 599-8570, Japan.
E-mail address: h-ikeno@21c.osakafu-u.ac.jp.

https://doi.org/10.1016/j.jcp.2017.11.016
0021-9991/

$$\tilde{\psi}(\boldsymbol{k}) = \int e^{-i\boldsymbol{k}\cdot r}\psi(\boldsymbol{r})d\boldsymbol{r} = 4\pi(-i)^l \tilde{f}_l(k)Y_{lm}(\hat{\boldsymbol{k}}), \tag{3}$$

where $\tilde{f}_l(k)$ is expressed as SBT given in (1). Since the spherical Bessel function $j_l(r)$ is defined in terms of Bessel function $J_\nu(r)$ of half-integer order as,

$$j_l(r) = \sqrt{\frac{\pi}{2x}} J_{l+\frac{1}{2}}(r), \tag{4}$$

a SBT can be regarded as a special case of *a Hankel transform* (HT) defined as,

$$\tilde{g}(k) = \int_0^\infty rg(r)J_\nu(kr)dr \quad (k > 0). \tag{5}$$

Both HT and SBT are used in many field, including astronomy, optics, electromagnetics, seismology, and quantum mechanics. In particular, SBT is involved in the scattering in atomic or nuclear systems [1], and multi-center integrals arises in atomic and molecular integrals [2].

The straight forward evaluation of integral (1) using conventional numerical integration method, such as the Gauss–Laguerre rule, meets intractable difficulties when k becomes large, because the integrand is highly oscillatory. Several approaches to overcome the difficulty have been proposed. The most efficient approach is the fast SBT method, where the transform is made on a logarithmic mesh for both the r and k in conjunction with variable transformation [3–7]. The integration is performed by two successive application of the fast Fourier transform (FFT). One of the drawback of this approach is the use of logarithmic mesh that most of mesh points are concentrated close to the origin. The fast SBT algorithm on linearly spaced mesh has also developed, where the integral representation of the spherical Bessel function $j_l(r)$ in terms of the Legendre polynomial is used with variable transformation, and the integral is performed via FFT [8]. In these two methods, the values of integral (1) on the predefined mesh points (either logarithmic or linear mesh) can efficiently be evaluated in $O(N \log N)$ operations. On the other hand, an appropriate interpolation or extrapolation is necessary to obtain the integral value for arbitrary points other than the mesh points on real axis. The numerical method for SBT in another direction is to partition the integral (1) into the integrals over subintervals between the zeros of spherical Bessel functions. The integrals on subintervals form an alternating series and can be summed with acceleration method. The advantage of this approach is that one can control the accuracy by adjusting the quadrature points. The drawback is, however, that the computational cost is much higher than that of fast SBT, as the integration has to be performed each value of k. See ref. [9] for the detailed comparison of the performance between these two approaches. Alternative approach for HT using wavelets was also proposed [10,11]. But the method is for HT with integer order and hence it cannot be directly applied to evaluate SBT.

In this paper, a new method for numerical evaluation of SBT at arbitrary points in high accuracy is proposed. The basic idea behind is to fit the integrand $r^2 f(r)$ by sum of analytic functions so that the SBT in (1) can be obtained analytically. The HT algorithm with the similar mind has already reported, where the function $rg(r)$ in (5) is fitted by sum of exponential type functions [12,13]. In our approach, the oscillatory spherical Bessel kernel $j_l(kr)$ is also approximated by an exponential sum with complex parameters. This enable us to evaluate SBT analytically at arbitrary points in half-open interval. The advantage of the present method compared to those in refs. [12,13] is that $r^2 f(r)$ can be expanded by various kind of analytic functions, including algebraic functions, trigonometric functions, exponential functions and combinations of them, as long as $r^2 f(r)e^{-ar}$ can be integrated analytically.

This paper is organized as follows. The theoretical background for the approximation of spherical Bessel kernel via an exponential sum is explained in Sec. 2. The details of the numerical algorithm to obtain exponential sum approximation of spherical Bessel functions numerically is described in Sec. 3.1 and 3.2. The procedure to obtain exponential sum approximation of residual part $r^2 f(r)$ is briefly explained and some results of numerical tests are provided in Sec. 3.3.

2. Exponential sum approximation of spherical Bessel functions

In this section, we are considering the approximation of spherical Bessel kernel $j_l(r)$ by an exponential sum. Let $g(r)$ be a function of the form,

$$g(r) = \sum_{k=1}^{N} c_k e^{-a_k r} \quad (r \geq 0), \tag{6}$$

where $a_k \in \mathbb{C}$, $Re(a_k) > 0$ are distinct complex numbers, and $c_k \in \mathbb{C} \setminus \{0\}$. The function $g(r)$ is a smooth, exponentially decaying function, and it oscillates if $Im(a_k) \neq 0$. Our problem here is to find parameters a_k and c_k with small number of terms M, such that

$$\left| j_l(r) - g(r) \right| < \epsilon \quad (r \geq 0) \tag{7}$$

where $\epsilon > 0$ is a prescribed accuracy of the approximation.

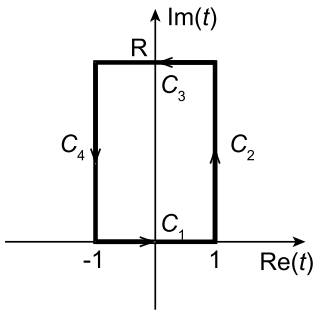

Fig. 1. Contour paths in the complex t-plane used for discretizing the integral representations of and spherical Bessel functions $j_l(r)$ with $r \in \mathbb{R}$.

Approximating analytic functions by exponential sums has been studied in applied mathematics. One of the most useful approaches to obtain an exponential sum approximation is to discretize the integral representation by using a numerical quadrature rule [14,15]. To obtain the exponential sum approximation of spherical Bessel function $j_l(r)$, let us consider the following integral representation,

$$j_l(r) = \frac{(-i)^l}{2} \int_{-1}^{1} e^{irt} P_l(t) dt, \tag{8}$$

where $P_l(t)$ is the Legendre polynomial of degree l. The integrand of (8) becomes highly oscillatory when r is large (see, Fig. 2(a)). Hence, the application of conventional quadrature rule, such as the Gauss–Legendre rule, on (8) is inefficient. Several quadrature rules for Fourier type integrals have been reported [16–18]. Unfortunately, in those quadrature rules, the quadrature nodes are chosen depending on the argument r, hence, they cannot be used for the present purpose. A common approach to remove the difficulty in the integration coming from the highly oscillatory nature of function is *the steepest descent method* [19,20]. In this approach, the integral is extended on complex plane and deform the contour paths so that the integrand decays rapidly. In this work, the method was applied to the integral representation in (8).

Let u, v be the real and imaginary part of t, so that $t = u + iv$, and consider the contour paths, $C_1 : t = u$, $u \in [-1, 1]$, $C_2 : t = 1 + iv$, $v \in [0, R]$, $C_3 : t = u + iR$, $u \in [-1, 1]$, and $C_4 : t = -1 + iv$, $v \in [0, R]$ with $R > 0$. Those four paths on the complex t-plane are shown in Fig. 1. C_1 coincides with the integration domain on real axis in (8). C_2 and C_4 are chosen to be the steepest descent paths. Along the paths the exponential term $e^{ixt} = e^{-xv} e^{\pm ix}$ rapidly decrease as parameter v increase and does not oscillate. According to the Cauchy's integral theorem,

$$\oint_{C_1+C_2+C_3+C_4} e^{irt} P_l(t) dt = 0, \tag{9}$$

for the closed contour constructed of those paths. Thus, the integral representation of the spherical Bessel function can be reformulated as

$$j_l(r) = -\frac{(-i)^l}{2} \int_{C_2+C_3+C_4} e^{irt} P_l(t) dt \equiv S_2(r) + S_3(r) + S_4(r), \tag{10}$$

where,

$$S_2(r) = -\frac{(-i)^{l+1}}{2} \int_0^R e^{-(v+i)r} P_l(-1+iv) dv = (-1)^{l+1} S_4^*(r), \tag{11a}$$

and

$$S_3(r) = \frac{(-i)^l}{2} \int_{-1}^{1} e^{-(R-iu)r} P_l(u+iR) du. \tag{11b}$$

As $P_l(-x) = (-1)^l P_l(x)$, the integral $S_3(r)$ can be split into two part,

$$S_3(r) = S_3'(r) + (-1)^l S_3'^*(r), \tag{11c}$$

with

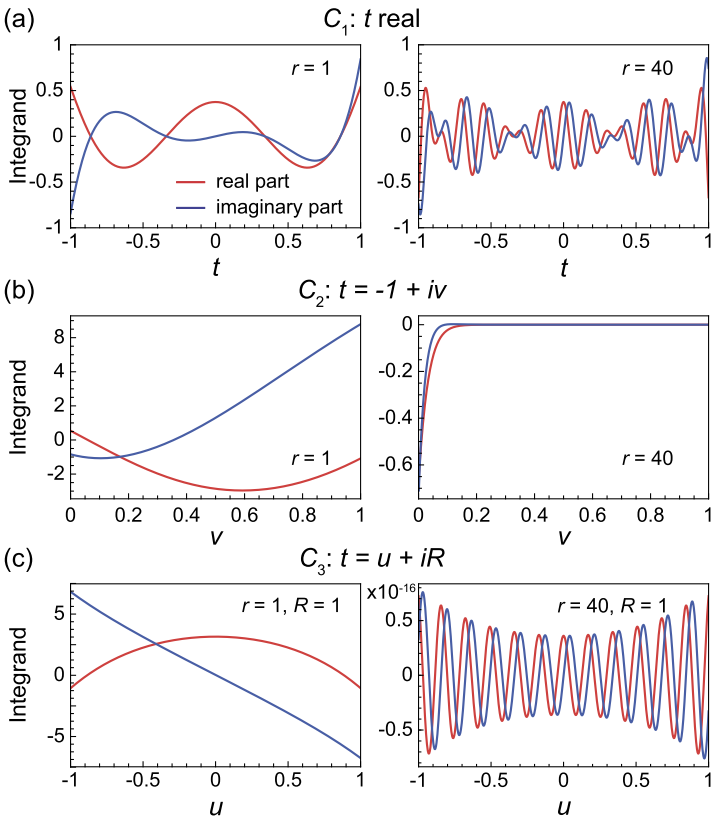

Fig. 2. Integrand for the integral representations of spherical Bessel function $j_4(r)$ for $r = 1$ and $r = 40$ along the contour paths C_1, C_2 and C_3 shown in Fig. 1. Real and imaginary part of integrands are drawn in red and blue lines, respectively. (For interpretation of the colors in this figure, the reader is referred to the web version of this article.)

$$S_3'(r) = \frac{(-i)^l}{2} \int_0^1 e^{-(R-iu)r} P_l(u+iR)du, \tag{11d}$$

so that

$$j_l(r) = S_2(r) + (-1)^{l+1} S_2^*(r) + S_3'(r) + (-1)^l S_3'^*(r). \tag{12}$$

The behavior of integrands in (8), (11a), and (11b) for $r = 1$ and $r = 40$ with $R = 1$ are shown in Fig. 2. For $r = 1$, integrands are smooth and hardly oscillate along all paths.

As mentioned before, the integrand on real axis (C_1) in (8) is highly oscillatory for $r = 40$. The oscillation disappears along the path C_2 as can be seen the right panel in Fig. 2(b). The integrand of $S_3(r)$ for $r = 40$ is highly oscillating. However, the magnitude of the integrand becomes negligibly small when r and R are significantly large, because of the presence of the factor e^{-Rr}. The contribution of $S_3(r)$ on $j_l(r)$ is negligibly small for large argument r. Following the observations, the integral (11a) and (11d) can be approximated using a quadrature rule as,

$$S_2(r) \approx -\frac{(-i)^{l+1}}{2} \sum_{j=1}^{N_2} w_j^{(2)} P_l\left(-1 + iy_j^{(2)}\right) e^{-(y_j^{(2)}+i)r}, \tag{13a}$$

and

$$S_3'(r) \approx \frac{(-i)^l}{2} \sum_{j=1}^{N_3} w_j^{(3)} P_l\left(y_j^{(3)} + iR\right) e^{-(R+iy_j^{(3)})r}, \tag{13b}$$

where $y_j^{(k)}$ and $w_j^{(k)}$ are nodes and weights of the quadrature rule. The details for selecting quadrature nodes and weights will be discussed in the next section. The approximation (13a) and (13b) have the form of exponential sum in (6). The exponential sum approximation of the spherical Bessel function can be obtained by substituting (13a) and (13b) into (12).

It should be noted that the integral $S_3(r)$ vanishes as $R \to \infty$ due to the factor e^{-Rr}. Thus, the spherical Bessel function can, in principle, be represented as sum of two integrals $S_2(r)$ and $S_4(r)$ on the steepest descent paths. In practice, however, we may suffer from large numerical round of error for evaluating the summation in (13a) when R becomes large, since the magnitude of the weight factor $P_l(-1+iy)$ may vary in wide range from 0 to R^l. In order to avoid this problem, $S_3(r)$ should be explicitly included to construct exponential sum approximation with keeping R as small as possible. How to choose the parameter R will be explained in the next section.

3. Details of numerical procedures

3.1. Discretization of integral representation for $j_l(r)$

As explained in the previous section, the exponential approximation of spherical Bessel function $j_l(r)$ can be obtained by discretizing the integral representation in the complex plane using appropriate quadrature rule, as described in (12) and (13). The choice of quadrature rule is crucial to achieve the approximation $g(r)$ satisfying (7) in high accuracy. The behavior of the integrand of $S_2(r)$ and $S_3'(r)$ significantly depend on the magnitude of argument r, as can be seen in Fig. 2. When r is small, the integrands of $S_2(r)$ and $S_3'(r)$ are both smooth functions and have significant contribution on entire region of integrals. When r is large, the contribution of $S_3'(r)$ becomes negligibly small in whole region because of the presence of e^{-Rr} factor. Thus, the contribution of $S_2(r)$ is dominating. In addition, the integrand of $S_2(r)$ has significant contribution near the end point $v = Im(t) = 0$ $(t = -1)$, and is decaying exponentially as v increases, as can be seen in Fig. 2(b). These observations suggest that many quadrature points should be distributed near the lower bound of integral region in order to achieve the approximation in high accuracy for large r. The Gauss–Legendre rule, which is most common quadrature rule for integral in finite interval, do not fulfill this requirement. This is confirmed by numerical experiments, where 500 points Gauss–Legendre rule were applied for evaluating integrals $S_2(r)$ and $S_3'(r)$. We found that the absolute errors of the exponential sum approximation for $j_l(r)$ $(0 \le l \le 10)$ are about order of 10^{-7} (only 1 or 2-digit accuracy) for $r > 10^5$.

In the present work, the double-exponential transformation formula for the numerical integration was adopted [21]. In this formula, an integral over $[-1, 1]$ can be approximated as

$$I = \int_{-1}^{1} f(x)dx \approx h \sum_{k=-N_-}^{N_+} w_k f(x_k), \tag{14a}$$

where

$$x_k = \tanh\left(\frac{\pi}{2}\sinh kh\right), \qquad w_k = \frac{\frac{\pi}{2}\cosh kh}{\cosh^2(\frac{\pi}{2}\sinh kh)}. \tag{14b}$$

The formula gives very high accuracy with small number of quadrature nodes, even if $f(x)$ is singular at the end points. For a given number of quadrature nodes $N = N_- + N_+ + 1$ interval $h > 0$ is chosen so that quadrature weights at the end points w_{N_-}, w_{N_+} become smaller than prescribed threshold $0 < \eta \ll 1$, i.e.,

$$h \approx \frac{1}{N}\ln\left[\frac{2}{\pi}\ln\left(\frac{4}{\pi\eta}\ln\frac{2}{\eta}\right)\right]. \tag{15}$$

We set $\eta = \epsilon_M / N_i$ for evaluating quadrature form (13a) and (13b), where ϵ_M is the machine epsilon.

The choice of parameter $R > 0$, the upper bound of $\mathrm{Im}(t)$ on contour paths, is also important to achieve the exponential sum approximation of $j_l(r)$ in high accuracy. R should be large enough so that the contribution of integrals $S_3(r)$ is negligibly small for large r where the integrand is highly oscillating. On the other hand, R should be kept small as possible so as not to increase the magnitude of Legendre polynomial in the weight factor in (13) significantly: otherwise, the summations in (13) become inaccurate especially for $r < 1$ because of the numerical round-off error.

The number of quadrature nodes N_2, N_3, and the parameter R were determined empirically, so that maximum absolute error becomes smaller than tolerance, ϵ_{tol}, for any $r > 0$. In the present work, computation was done in double precision with $\epsilon_{\mathrm{tol}} = 10^{-13}$. The parameters were set to be $N_2 = 200, N_3 = 120 + 2l$, and $R = 5/(l+1)$ respectively. By selecting the parameters in this way, the exponential sum approximation of $j_l(r)$ with maximum absolute error smaller than 5×10^{-14} can be obtained for l up to ten.

3.2. Reduction of terms

The exponential sum approximation of $j_l(r)$ obtained by the procedure described above can be approximated with another exponential sum with smaller number of terms, such that,

$$\tilde{g}(r) = \sum_{k=1}^{M} \tilde{c}_k e^{-\tilde{a}_k r}, \quad \left|g(r) - \tilde{g}(r)\right| < \epsilon, \tag{16}$$

Table 1
Summary of the exponential sum approximation for $j_l(r)$. M represents the number of terms after applying the modified balanced truncation with accuracy $\epsilon = 10^{-12}$. $\epsilon_{\max}$ and ϵ_{ave} are the maximum and averaged error on the 10^6 points logarithmically spaced grid on $[10^{-5}, 10^7]$.

l	M	$\epsilon_{\max}$	ϵ_{ave}
0	130	7.0×10^{-13}	3.3×10^{-13}
1	132	4.2×10^{-13}	1.4×10^{-13}
2	134	7.1×10^{-13}	3.1×10^{-13}
3	136	4.4×10^{-13}	2.4×10^{-13}
4	136	3.0×10^{-13}	1.7×10^{-13}
5	138	8.8×10^{-13}	4.0×10^{-13}

with $M < N$. Numerical procedures finding shorter exponential sum approximation in (16) based on the theory of Adamjan, Arov, and Krein (AAK theory) has been discussed in literatures [22–24]. Alternatively, the balanced truncation method, which is an algorithm use for model order reduction, can also be used [25,26].

In this work, a modified balanced truncation method for sparse exponential sum approximation was adopted. In this method, we consider the Laplace transform of exponential sum in (6),

$$G(s) = \mathcal{L}\big[g(r)\big] = \int_0^\infty e^{-sr} g(r) dr = \sum_{k=1}^{N} \frac{c_k}{s + a_k}, \tag{17}$$

and find approximation $\tilde{G}(s) = \mathcal{L}[\tilde{g}(r)]$ such that $|G(s) - \tilde{G}(s)| < \epsilon$. $G(s)$ can be written in matrix form as,

$$G(s) = C(sI + A)^{-1} B, \tag{18}$$

where $A = \text{diag}(a_1, a_2, \ldots, a_N) \in \mathbb{C}^{N\times N}$, $B = (\sqrt{c_1}, \sqrt{c_2}, \ldots, \sqrt{c_N})^T \in \mathbb{C}^{N\times 1}$ and $C = B^T$. Using the terminology of control theory, $G(s)$ is a transfer function of a linear time-invariant system identified by matrices $(A,\ B,\ C)$. The balanced truncation method finds approximation of the system with lower order matrices $(T^{-1}AT, T^{-1}B,\ CT)$. Here, $T \in \mathbb{C}^{M\times N} (M < N)$ is a projection matrix which is determined from the singular vectors of Gramian matrices P and Q, which are solutions of equations, $AP + PA^* = BB^*$ and $AQ + QA^* = C^*C$, respectively. Because of the diagonal structure of A, elements of matrices P, Q can be obtained analytically as,

$$P_{ij} = \frac{\sqrt{c_i c_j^*}}{a_i + a_j^*} = Q_{ij}^*. \tag{19}$$

Thus, P, Q are Hermitian, quasi-Cauchy matrices. The algorithms for computing singular value decomposition of a quasi-Cauchy matrix in high accuracy is available [27–29]. In this work, the con-eigenvalue decomposition $P = \overline{U}\Sigma U^T$ with $UU^T = I$, that is a special case of singular value decomposition, of a quasi-Cauchy matrix is computed using the algorithm proposed by Haut and Beylkin [30]. The number of terms, M, in truncated exponential sum (16) is determined from the con-eigenvalues, so that $\sigma_{M+1} < \epsilon$. By setting the projection matrix $T = U[1:N, 1:M]^H$, the exponents $\tilde{a}_k$ are obtained from the eigenvalue decomposition $T^{-1}AT = X\Lambda X^T$ as $\Lambda = diag(\tilde{a}_1, \tilde{a}_2, \ldots, \tilde{a}_M)$. The corresponding coefficients c_k are obtained as $X^T T^{-1} B = (\sqrt{\tilde{c}_1}, \sqrt{\tilde{c}_2}, \ldots, \sqrt{\tilde{c}_M})^T$. More details about the balanced truncation method used in this work will be published elsewhere.

Using the procedure above, the exponential sum approximation of $j_l(r)$ was obtained. Fig. 3 shows the results of exponential sum approximation for $j_4(r)$ with accuracy $\epsilon = 10^{-12}$. The 136-terms approximation was obtained by the modified balanced truncation. The nodes $z_k = e^{-a_k}$ and coefficients c_k on complex plane, and absolute errors on $r \in [10^{-5}, 10^7]$ are shown. The absolute errors of approximation are smaller than the prescribed accuracy ϵ for all $r \geq 0$. The exponential sum approximation of other spherical Bessel functions with various l are summarized in Table 1. The number of terms M, maximum $(\epsilon_{\max})$ and averaged (ϵ_{ave}) absolute errors on the 10^6 points logarithmically spaced grid in $[10^{-5}, 10^7]$ are shown. The parameters a_k and c_k for exponential sum approximations of $j_l(r)$ for $0 \leq l \leq 10$ are also given in supplemental material.

3.3. Exponential sum approximation of residual function

Using the obtained exponential sum approximation of $j_l(r)$, SBT can be evaluated analytically as long as integral of $r^2 f(r) e^{-pr}$ on half-open interval can be obtained analytically. Here, we consider the approximation of $r^2 f(r)$ by sum of exponential functions multiplied by power function, given as

$$r^2 f(r) = r^n \sum_{i=1}^{N} \gamma_i e^{-\alpha_i r}, \tag{20}$$

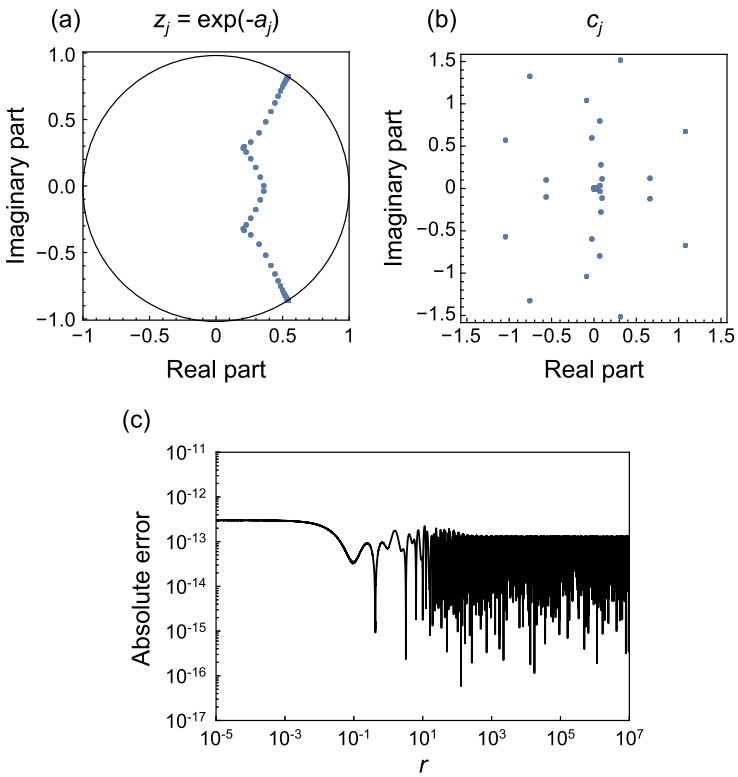

Fig. 3. Results of the exponential sum approximation of spherical Bessel function $j_4(r)$. (a) Distribution of $z_j = \exp(-a_j)$ for exponential sum. (b) Distribution of coefficients c_j. (c) Absolute error of the exponential sum approximation on $r \in [10^{-5}, 10^7]$.

where $n > -1, \alpha_i \in \mathbb{C}, Re(\alpha_i) > 0$ are distinct complex numbers, and $\gamma_i \in \mathbb{C} \setminus \{0\}$. The approximation of the form (20) can be obtained by sampling $r^{2-n} f(r)$ on uniform grid and applying Prony-like methods. The methods are well established and commonly used in the field of signal processing, hence, are not explained here. We just refer to [31–33] for details about the Prony-like methods.

Once the parameters in (20) are obtained, the SBT of $f(r)$ can be analytically obtained in terms of Gauss hypergeometric functions ${}_2F_1$ with complex arguments as (see, 6.621.1 of [34]),

$$\begin{aligned}\tilde{f}_{l,n}(k) &= \sum_{i=1}^{N} \gamma_i \int_0^\infty r^n e^{-\alpha_i r} j_l(kr) dr \\ &= \sqrt{\frac{\pi}{2}} \sum_{i=1}^{N} \gamma_i \frac{\Gamma(l+n+1)}{(2l+1)!!} \frac{k^l}{\alpha_i^{l+n+1}} \times {}_2F_1\left(\frac{l+n+1}{2}, \frac{l+n+2}{2}; l+\frac{3}{2}; -\frac{k^2}{\alpha_i^2}\right). \end{aligned} \tag{21}$$

However, the numerical evaluation of hypergeometric function for complex arguments is still not an easy task [35–37]. This can be avoided by utilizing the exponential sum approximation of $j_l(r)$. By substituting $j_l(r) \approx \sum_{m=1}^{M} c_m \exp(-a_m r)$ to (21), we obtain the approximation of $\tilde{f}_{l,n}(k)$ as

$$\tilde{f}_{l,n}(k) \approx \tilde{g}_{l,n}(k) = n! \sum_{i=1}^{N} \sum_{m=1}^{M} \frac{c_m \gamma_i}{(a_m k + \alpha_i)^{n+1}}. \tag{22}$$

By using (22), the SBT can be evaluated efficiently as a sum of rational functions.

3.4. Numerical examples

In this section, we present some numerical examples to demonstrate the performance of our SBT algorithm via exponential sum approximation. In order to test the accuracy of the SBT of exponential sum function (19), it is sufficient to consider the case of $N = 1$, such as,

$$f(r) = r^{n-2} e^{-\alpha r}. \tag{23}$$

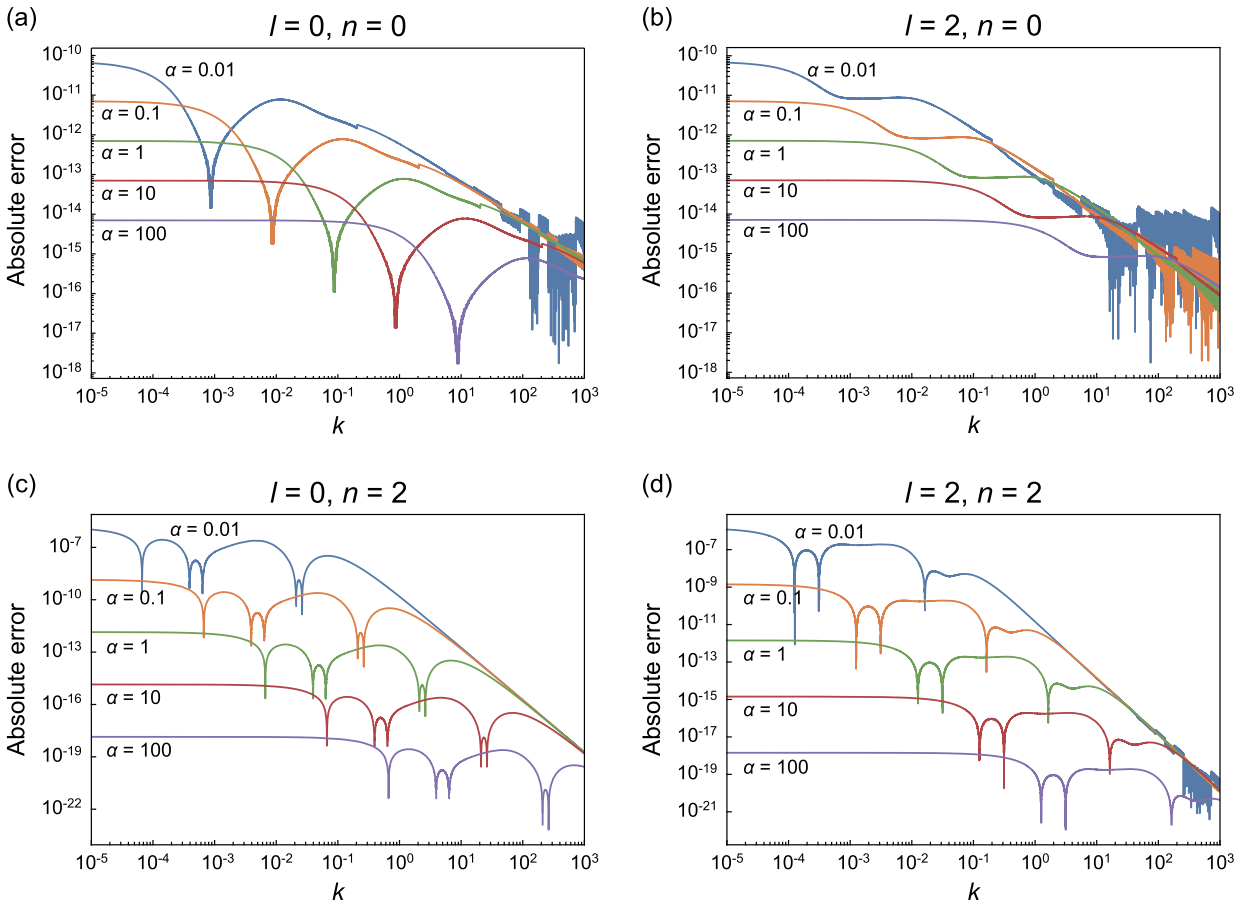

Fig. 4. Absolute errors $|\tilde{f}_{n,l}(k) - \tilde{g}_{n,l}(k)|$ of spherical Bessel transform of $f(r) = r^{n-2}e^{-\alpha r}$ with $\alpha = 0.01, 0.1, 1, 10, 100$.

The SBT of function (23) was evaluated using exact formula (21) and approximation (22) with varying exponents α. The absolute errors $|\tilde{f}_{l,n}(k) - \tilde{g}_{l,n}(k)|$ for $(l, n) = (0, 0), (2, 0), (0, 2), (2, 2)$, and $\alpha = 0.01, 0.1, 1, 10, 100$ on the interval $k \in [10^{-5}, 10^{5}]$ are shown in Fig. 4. The hypergeometric function in (21) is evaluated using arbitrary precision arithmetic, using the `'mpmath'` Python library. For evaluation of (22), 130 and 134 terms exponential sum approximations are used for spherical Bessel kernel $j_0(kr)$ and $j_2(kr)$, respectively. In all the cases, the absolute error tends to increase as k decreases to zero. In addition, the smaller the exponent parameter α, the larger the absolute error close to $k = 0$. This is because the factor $(a_m k + \alpha)^{-n-1}$ in (22) become significantly large when k and α are small and enhance the numerical round off error of exponential sum. However, the approximation error shown in Fig. 4 would be acceptable for applications in many physical problems.

Similar calculations were performed with complex exponent parameters. Fig. 5 shows absolute errors $|\tilde{f}_{l,n}(k) - \tilde{g}_{l,n}(k)|$ for $(l, n) = (0, 0), (2, 0)$, and with $\alpha = e^{i\varphi}$ $(\varphi = 0, \pi/6, \pi/4, \pi/3)$. The results suggest that the absolute errors do not strongly depend on the argument of α. The errors are kept in same order as long as the magnitude of parameter α is same.

The range of the magnitudes of α_i is strongly depend on feature of function $f(r)$. In the case of Gaussian distribution function, i.e., $f(r) = \mathrm{e}^{-r^2/2\sigma^2}$, for instance, $r^2 f(r)$ can be approximated using a Prony-like method by a 17 terms exponential sum with an accuracy of 10^{-13} on $r \geq 0$, where the magnitude of α_i is in $3.32/\sigma < |\alpha_i| < 6.81/\sigma$. Thus, the SBT can be evaluated in good accuracy using the exponential sum approximation for modest values of σ. The $|\alpha_i|$ varies much wider range when $f(r)$ is singular at origin and slowly decaying. For instance, the exponential sum approximation of the power function, $r^2 f(r) = r^{-\beta}$ $(\beta > 0)$, in the finite interval $[\delta, 1]$ $(\delta > 0)$ can be obtained in accordance with the procedure developed by Beylkin and Monzón [14]. A 137 terms approximation is obtained for $\beta = -2$ and $\delta = 10^{-10}$ with the relative accuracy of 10^{-10}. The parameter α_i are all positive real values and are in $0.05 < \alpha_i < 8.5 \times 10^{13}$. This implies that the SBT can be evaluated in good accuracy by using the proposed algorithm even if the function $f(r)$ has $r^{-\beta}$ singularity.

Exponential functions of the form (23) are frequently used in quantum chemistry, where an atomic orbital is expressed as linear combinations of Slater-type orbitals (STOs) as $\chi_{nlm}(\boldsymbol{r}) = \sum_i c_i r^n e^{-\alpha_i r} Y_{lm}(\hat{\boldsymbol{r}})$. The number of terms is typically two to four per each atomic orbital. The power factor n, which represents the principal quantum number of atomic orbitals, varies from one to seven, depending on atomic species. The exponents α_i are predetermined to reproduce the electronic structures of atoms and molecules, which exceeds 0.4 for all the atoms [38,39]. Hence the SBTs of STOs can also be evaluated

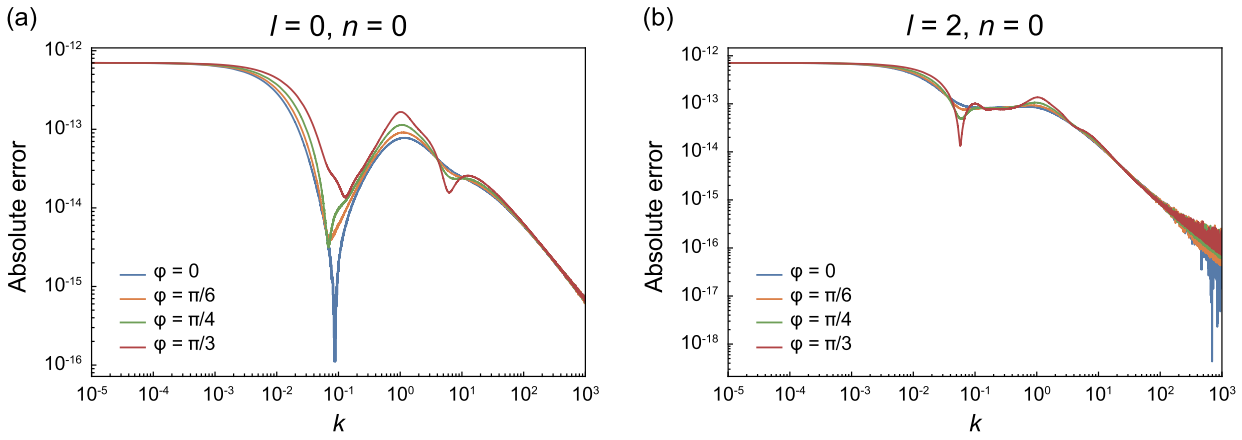

Fig. 5. Absolute errors $|\tilde{f}_{n,l}(k) - \tilde{g}_{n,l}(k)|$ of spherical Bessel transform of $f(r) = r^{n-2}e^{-\alpha r}$ with complex exponents, $\alpha = e^{i\varphi}$ $(\varphi = 0, \pi/6, \pi/4, \pi/3)$.

efficiently and accurately, which would be useful to evaluate the multicenter integrals between STOs required to construct Hamiltonian matrix [40,41].

3.5. Computational costs

Finally, we discuss the computational cost of the proposed algorithm for the numerical evaluation of the SBT. The computation of the parameters for the exponential sum approximation of spherical Bessel function ($j_l(r)$) takes some time (about ten seconds using modern CPU), especially for reducing the number of terms by the modified balanced truncation method as matrix decompositions and multiplications are required. However, the parameters for $j_l(r)$ can be precomputed and reused for evaluating the many SBTs, hence, the computational costs for this step could be negligible for practical use. The computational cost for the exponential sum approximation of the residual functions ($r^2 f(r)$) is hard to estimate: it strongly depends on the nature of the function, e.g., the decay rate or the presence of singularity. If $r^2 f(r)$ is smooth, non-singular and rapidly decaying function, the exponential sum approximation can be obtained within a second using the Prony-like methods.

The evaluation of a SBT using (22) requires $O(MN)$ operations for each k, where M and N are number of terms for the exponential sum approximations of $j_l(r)$ and $r^2 f(r)$, respectively. The values of M are summarized in Table 1, which can be reduced if larger absolute error for the approximation of $j_l(r)$ is acceptable. The value of N strongly depends on the feature of $f(r)$. If $r^2 f(r)$ is sooth and rapidly decaying, the function can be well approximated by several tens of exponential functions (e.g., $N = 15$ for the Gaussian distribution function with the accuracy of 10^{-13}). In typical case, MN is about order of one thousand.

Because the parameters for the exponential sum approximation of $j_l(r)$ are complex numbers, the use of complex arithmetic cannot be avoided at the last step. This results in a loss of computational efficiency because the computational cost of complex arithmetic is about four times larger than that of real arithmetic. The SBT can also be evaluated in high accuracy using real arithmetic by applying adaptive integration to evaluate the integral (1) directly. However, the latter approach becomes inefficient when we evaluate the SBT at large k, as the number of integration points required to achieve the desired accuracy increases significantly. To demonstrate this behavior, the SBT of singe exponential function given in (23) was also evaluated for $n = 0$ and $l = 2$ using QUADPACK, a subroutine package for automatic integration, at selected values of k. The numbers of integration points required to achieve the accuracy of 10^{-12} is 315, 1155, 4935, and 9513 at $k = 1$, 10, 50, and 100, respectively. In the proposed method, in contrast, the SBT can be obtained as a sum of $132N$ terms rational functions in (22). The computational cost of the proposed algorithm for evaluating the SBT is independent of the magnitude of k, and hence, would be much more efficient than adaptive integration scheme at large k.

4. Summary

In this paper, a new algorithm for numerically evaluating SBT in high accuracy was proposed. In this approach, both the spherical Bessel kernel, $j_l(kr)$, and residual part of integrand, $r^2 f(r)$, were approximated by exponential sums in the form (6) and (19). Then, the SBT was evaluated analytically as a sum of rational function in (22).

The procedures to obtain the exponential sum approximation of $j_l(r)$ were described in detail. Starting from the integral representation of $j_l(r)$ in (8), the variable of integration was extended in complex plane, and integration paths were modified along the steepest descent paths, as shown in Fig. 1. The integral representations on those paths were discretized using the double-exponential transformation formula for numerical quadrature. Then, the optimal exponential sum with smaller number of terms was obtained using modified balanced truncation algorithm.

Once the exponential sum approximation of $r^2 f(r)$ is obtained, the SBT of $f(r)$ at arbitrary points on $k \geq 0$ can be evaluated efficiently. The numerical results in Sec. 3.4 confirmed that the SBT can be obtained in high accuracy, except the case that both the magnitude of exponents and k are too small.

The present approach can also be extended to evaluate SBT when $f(r)$ is expressed as sum of other type of analytic functions, including trigonometric and algebraic functions, as long as $r^2 f(r)e^{-ar}$ can be evaluated efficiently and in high accuracy. This technique could be applied, for instance, the evaluation of multi-center integrals between atomic orbitals in quantum chemistry. The multi-center integrals can be obtained by performing forward SBTs of atomic orbitals, multiplying them, and then, performing backward SBT [2,42], which could be evaluated efficiently by applying the Prony-like method for fitting radial functions as exponential sums. Further research in this direction is now in progress.

Acknowledgements

This work was supported by PRESTO, Grant no. JPMJPR16N1 16815006 from Japan Science and Technology Agency (JST), and the Grant-in-Aid for Scientific Research on Innovative Areas, Grant No. 26106518 from the Ministry of Education, Culture, Sports, Science and Technology (MEXT) of Japan.

Appendix A. Supplementary material

Supplementary material related to this article can be found online at https://doi.org/10.1016/j.jcp.2017.11.016.

References

[1] A.E. Glassgold, G. Ialongo, Phys. Rev. 175 (1968) 151–159.
[2] J.D. Talman, Int. J. Quant. Chem. 93 (2003) 72–90.
[3] W.L. Anderson, ACM Trans. Math. Softw. 8 (1982) 344–368.
[4] P. Koval, J.D. Talman, Comput. Phys. Commun. 181 (2010) 2212–2213.
[5] A.E. Siegman, Opt. Lett. 1 (1977) 13–15.
[6] J.D. Talman, Comput. Phys. Commun. 30 (1983) 93–99.
[7] J.D. Talman, Comput. Phys. Commun. 180 (2009) 332–338.
[8] M. Toyoda, T. Ozaki, Comput. Phys. Commun. 181 (2010) 277–282.
[9] K. Key, Geophysics 77 (2012) F21–F30.
[10] R.K. Pandey, V.K. Singh, O.P. Singh, Commun. Comput. Phys. 8 (2010) 351–373.
[11] V.K. Singh, O.P. Singh, R.K. Pandey, Comput. Phys. Commun. 179 (2008) 812–818.
[12] P.K. Gupta, S. Niwas, N. Chaudhary, J. Earth Syst. Sci. 115 (2006) 267–276.
[13] H. Zhang, Y. Chen, X. Nie, J. Appl. Math. 2014 (2014) 105469.
[14] G. Beylkin, L. Monzón, Appl. Comput. Harmon. Anal. 28 (2010) 131–149.
[15] L. Monzón, G. Beylkin, Discrete Contin. Dyn. Syst. 36 (2016) 4077–4100.
[16] T. Ooura, M. Mori, J. Comput. Appl. Math. 38 (1991) 353–360.
[17] T. Ooura, M. Mori, J. Comput. Appl. Math. 112 (1999) 229–241.
[18] K. Tanaka, J. Comput. Appl. Math. 266 (2014) 73–86.
[19] D. Huybrechs, S. Vandewalle, SIAM J. Numer. Anal. 44 (2006) 1026–1048.
[20] A. Gil, J. Segura, N.M. Temme, Numer. Algorithms 33 (2003) 265–375.
[21] M. Mori, M. Sugihara, J. Comput. Appl. Math. 127 (2001) 287–296.
[22] G. Beylkin, L. Monzón, Appl. Comput. Harmon. Anal. 19 (2005) 17–48.
[23] F. Andersson, M. Carlsson, M.V. de Hoop, J. Approx. Theory 163 (2011) 213–248.
[24] G. Plonka, V. Pototskaia, arXiv:1609.09603 [math.NA], 2016.
[25] K. Xu, S. Jiang, J. Sci. Comput. 55 (2013) 16–39.
[26] W. McLean, arXiv:1606.00123 [math.NA], 2016.
[27] J. Demmel, SIAM J. Matrix Anal. Appl. 21 (1999) 562–580.
[28] J. Demmel, Accurate SVDs of Structured Matrices, Netlib, 1997.
[29] J. Demmel, M. Gu, S. Eisenstat, I. Slapničar, K. Veselić, Z. Drmač, Linear Algebra Appl. 299 (1999) 21–80.
[30] T.S. Haut, G. Beylkin, SIAM J. Matrix Anal. Appl. 33 (2012) 1101–1125.
[31] D. Potts, M. Tasche, Linear Algebra Appl. 439 (2013) 1024–1039.
[32] F. Filbir, H.N. Mhaskar, J. Prestin, Constr. Approx. 35 (2012) 323–343.
[33] D. Potts, M. Tasche, Appl. Numer. Math. 88 (2015) 31–45.
[34] D. Zwillinger (Ed.), Table of Integrals, Series, and Products, 8th ed., Academic Press, Boston, 2014.
[35] N. Michel, M.V. Stoitsov, Comput. Phys. Commun. 178 (2008) 535–551.
[36] J.A. Doornik, Math. Comput. 84 (2015) 1813–1833.
[37] J.W. Pearson, S. Olver, M.A. Porter, Numer. Algorithms 74 (2017) 821–866.
[38] E. van Lenthe, E.J. Baerends, J. Comput. Chem. 24 (2003) 1142–1156.
[39] E. Clementi, C. Roetti, At. Data Nucl. Data Tables 14 (1974) 177–478.
[40] P.E. Hoggan, M.B. Ruiz, T. Özdoğan, in: M.V. Putz (Ed.), Quantum Front. At. Mol., 1st ed., Nova Science Publishers, Inc., 2011, pp. 61–90.
[41] J.D. Talman, Int. J. Quant. Chem. 100 (2004) 109–113.
[42] M. Toyoda, T. Ozaki, J. Chem. Phys. 130 (2009) 124114.